PHYSICAL REVIEW B **95**, 115134 (2017)

Spin-entanglement between two freely propagating electrons: Experiment and theory

D. Vasilyev,[1] F. O. Schumann,[1] F. Giebels,[2] H. Gollisch,[2] J. Kirschner,[1] and R. Feder[1,2]
[1]*Max-Planck Institut für Mikrostrukturphysik, Weinberg 2, 06120 Halle, Germany*
[2]*Theoretische Festkörperphysik, Universität Duisburg-Essen, 47048 Duisburg, Germany*
(Received 7 April 2016; revised manuscript received 20 February 2017; published 17 March 2017)

Theory predicts that electron pairs, which are emitted from a crystalline surface upon impact of spin-polarized low-energy electrons, can be spin-entangled. We quantify this entanglement by the von Neumann entropy, which we show to be closely related to the spin polarization of the emitted electrons. Measurement of the spin polarization therefore facilitates an experimental study of the entanglement. As target we used a Cu(111) surface, which exhibits an electronic surface state giving rise to a high pair emission intensity. Experimental spin polarization spectra for several orientations of the reaction plane broadly agree with their theoretical counterparts. They are consistent with spin entanglement of the electron pair at a macroscopic distance.

DOI: 10.1103/PhysRevB.95.115134

I. INTRODUCTION

Quantum theory has proven to be a very accurate description of nature. Furthermore, modern technology rests on the understanding of the quantum properties of matter and we cite semiconductor technology and spintronics as specific examples. Right at the beginning of the formulation of quantum mechanics it was realized that it contains features which are seemingly at odds with fundamental views on the description of nature. This was expressed in a famous gedankenexperiment by Einstein-Podolsky-Rosen [1]. This led Schrödinger to introduce the term entanglement and we quote [2]: "When two systems enter into temporary physical interaction and when after a time of mutual influence the systems separate again, then they can no longer be described in the same way as before, viz. by endowing each of them with a representative of its own. I would not call that *one* but rather *the* characteristic trait of quantum mechanics. By the interaction the two representatives (or ψ functions) have become entangled."

The concept of entanglement plays a central role in current research activities covering diverse fields like quantum computing, cryptography, and teleportation to name a few. Consequently, a large body of work exists and we refer to a few reviews for more information [3–5]. An obvious scenario considered by Schrödinger constitutes the scattering of a primary particle with a target. Specifically, the scattering of two electrons interacting via the Coulomb interaction is regarded a source for entangled electron pairs. Such a process has so far been explored only theoretically, for collisions between two free electrons [6,7] and between a free electron and an electron bound in a crystal surface [8]. The latter process is also known as (e,2e) and has been shown to reveal important aspects in the electron correlation of atoms, molecules, and surfaces.

The degree of entanglement can be quantified in the von Neumann entropy [6]. We will show that this entity is related to the spin polarization of the emitted electrons in an (e,2e) process. This spin polarization is experimentally accessible and allows for an experimental test of entanglement. As a specific example we investigated in theory and experiment the (e,2e) process on a Cu(111) surface. It is well established that this surface exhibits a prominent surface state (cf. Ref. [9] and references therein). This state is confined into a small region near the Fermi level and near the center of the surface Brillouin zone. This facilitates identification of its contribution in the pair emission as demonstrated previously [10,11]. We study the spin entanglement in the electron pair emission from a Cu(111) surface. To this end, we use a spin-polarized electron source and a spin detector in one of the two electron trajectories. The present work reports the first experimental study for the entanglement of two electrons, which after the collision propagate freely in space over distances of order 10 cm.

II. EXPERIMENT

In Fig. 1, we sketch the basics of our experimental setup and the nomenclature we use. In an (e,2e) process, a primary electron e_1 hits a sample and interacts with a valence electron labeled e_2. This leads to the emission of a pair of electrons called e_3 and e_4, respectively. The experimental studies used a time-of-flight coincidence spectrometer with a pulsed spin-polarized electron gun as described previously [12]. The generation of a spin-polarized electron beam is an established technique. We use a strained AlInGaAs/AlGaAs superlattice with negative electron affinity excited by a pulsed laser diode with 828 nm wavelength [13]. The spin polarization is around 60%. The polarization vector is oriented orthogonal to the paper plane and is switched between the states "+" and "−" by reversal of the helicity of the light source. The primary beam propagates along the sample normal. The key modification of the setup was the rearrangement of the detector labeled B in Fig. 1. Before electrons e_3 can reach this detector, a transfer lens focusses them onto a spin-polarizing mirror [14–16]. Essentially, it consists of a pseudomorphic monolayer of Au on Ir(100) and we use the (0,0) beam in elastic reflection. The detectors A and B consist of channel plates with delay-line anodes. The information about the impact position and flight times allows to determine the kinetic energy and emission angles of the electrons e_3 and e_4.

We use as target a Cu(111) surface which was cleaned via Ar^+ sputtering and annealing. We have demonstrated in earlier (e,2e) experiments that the Shockley surface state makes a strong contribution to the intensity [10,11]. Suitable primary energies E_p are in the range 19–30 eV. The identification of this state is possible via energy and in-plane momentum conservation in the (e,2e) process as we explain in the

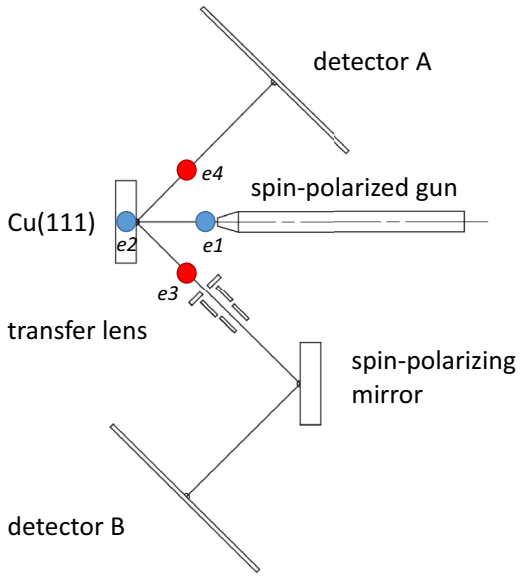

FIG. 1. A primary electron e_1 interacts with a valence electron e_2, this leads to the emission of electrons e_3 and e_4. The reaction plane is the paper plane and the spin polarization of the primary beam is perpendicular to it. The spin polarizing mirror measures the spin polarization of the emitted electron e_3 perpendicular to the scattering plane.

theoretical section. There we also discuss the usefulness of the Cu(111) surface state.

The key quantity to measure is the spin-polarization P_3 of electrons e_3 as a function of the energy difference $E_3 - E_4$ of the two emitted electrons. The spin analyzing properties of a spin-mirror depend critically on the angle of incidence and primary energy [14–16]. Good working parameters have been identified if the electron beam to be analyzed strikes the mirror with an angle of 45° with respect to the spin-mirror surface. The scattering energies are then around 11 or 50 eV. Due to geometrical constraints we could not adopt this scattering angle and had to identify other suitable conditions. For this we turned the Cu(111) surface by 22.5°, now the elastically reflected (0,0) beam from the Cu(111) surface passes through the transfer lens and serves as primary beam for the spin mirror. The spin-orbit interaction is weak in Cu, consequently, we can assume that the spin polarization of the primary beam is maintained upon reflection from the Cu(111) surface. From these preliminary investigations, we found an optimum if the incoming beam strikes the spin mirror at an angle of 35°. If the scattering energy is about 11 eV, the spin sensitivity S_{spin} adopts a value of 0.2 in contrast to 0.6 for an angle of 45° [16]. We denote the intensity I_+ and I_- for the coincidence measurement with primary spin "+" and "−". The term P_{gun} takes into account the spin polarization of the primary beam. With these definitions we determine the spin polarization P_3 as

$$P_3 = \frac{1}{P_{\text{gun}}} \frac{1}{S_{\text{spin}}} \frac{I_+ - I_-}{I_+ + I_-}. \tag{1}$$

III. THEORETICAL FORMALISM

A theoretical treatment of the creation of spin entanglement by (e,2e) and of its quantification by a modified von Neumann entropy has been put forward in Ref. [8]. It therefore suffices to recall the essential features and formulas.

The basic ingredients are four one-electron states, which in the absence of spin-orbit coupling (which can be neglected for the low-Z material Cu) can be written as a product of a spatial and a spin part: $|E_n,\vec{k}_n^{\parallel}\rangle|\sigma_n\rangle$, where E_n is the energy, $\vec{k}_n^{\parallel}$ the surface-parallel momentum, and $\sigma_n = +/-$ indicates the spin orientation (up/down) normal to the reaction plane. The index $n = 1$ refers to the incident electron, $n = 2$ to the valence electron, $n = 3$ to the outgoing electron labeled e_3 in Fig. 1, and $n = 4$ to the outgoing electron e_4. Energy and surface-parallel momentum (modulo a parallel reciprocal lattice vector) are conserved, i.e.,

$$E_1 + E_2 = E_3 + E_4 \quad \text{and} \quad \vec{k}_1^{\parallel} + \vec{k}_2^{\parallel} = \vec{k}_3^{\parallel} + \vec{k}_4^{\parallel}. \tag{2}$$

To make the following more transparent, we write the above four states as $|n,\sigma_n\rangle = |n\rangle|\sigma_n\rangle$ with $n = 1,\ldots,4$, where $|n\rangle$ stands for the spatial part $|E_n,\vec{k}_n^{\parallel}\rangle$.

We recall that these states are quasiparticle states, i.e., the influence of all the other electrons of the crystal is incorporated via a complex self-energy term in the one-electron potential. Since electrons in metals near the Fermi energy are adequately described within an independent quasiparticle picture, the valence state $|2,\sigma_2\rangle$ can—via energy and momentum conservation, cf. Eq. (2)—be singled out from the N-electron ground state and the remaining $(N-1)$-electron state plays no role in our (e,2e) formalism except for providing the screening of the Coulomb interaction between two quasielectrons.

Before addressing the initial and final two-electron states, which are built from these one-electron states, we briefly recall the concept of entanglement in the present case of two identical fermions, which has been discussed extensively in the literature (Refs. [6,17,18] and references therein). A two-electron state, which consists of a linear combination of N linearly independent Slater determinants (antisymmetrized products of one-electron states) with expansion coefficients a_k—with $k = 1,\ldots,N$—satisfying the normalization condition $\sum_k |a_k|^2 = 1$, is genuinely entangled, if N is greater than one. As quantitative measure of the entanglement of such a state we choose a modified von Neumann entropy:

$$S = -\sum_{k=1}^{N} |a_k|^2 \log_2(|a_k|^2). \tag{3}$$

A state consisting of a single Slater determinant is thus not entangled with $S = 0$. For entangled states, one has $S > 0$, with maximal value $S = 1$ reached in the case $N = 2$ and $|a_1|^2 = |a_2|^2 = 0.5$.

In (e,2e), the initial two-electron state is an antisymmetrized product of the incoming and valence one-electron states: $\frac{1}{\sqrt{2}}(|1,\sigma_1\rangle|2,\sigma_2\rangle - |2,\sigma_2\rangle|1,\sigma_1\rangle)$. Being just a single Slater determinant, this state is—for parallel as well as for antiparallel spins σ_1 and σ_2—not entangled and has entropy $S = 0$.

The final two-electron state differs for parallel and antiparallel spins. For the former ($\sigma := \sigma_3 = \sigma_4 = \pm$), it is

$$(f - g)\frac{1}{\sqrt{2}}(|3,\sigma\rangle|4,\sigma\rangle - |4,\sigma\rangle|3,\sigma\rangle), \tag{4}$$

where f and g are the direct and exchange transition matrix elements. Being just a single Slater determinant, this state is not entangled.

For antiparallel spins ($\sigma := \sigma_3 = \pm$ and $\bar{\sigma} := -\sigma = \sigma_4 = \mp$), the final two-electron state has the form

$$\frac{f}{\sqrt{2}}(|3,\sigma\rangle|4,\bar{\sigma}\rangle - |4,\bar{\sigma}\rangle|3,\sigma\rangle) - \frac{g}{\sqrt{2}}(|3,\bar{\sigma}\rangle|4,\sigma\rangle - |4,\sigma\rangle|3,\bar{\sigma}\rangle). \quad (5)$$

Consisting of two linearly independent Slater determinants, it is entangled with entropy [cf. Eq. (3)]

$$S = -|\tilde{f}|^2 \log_2 |\tilde{f}|^2 - |\tilde{g}|^2 \log_2 |\tilde{g}|^2, \quad (6)$$

where $\tilde{f} = f/(\sqrt{|f|^2 + |g|^2})$ and $\tilde{g} = g/(\sqrt{|f|^2 + |g|^2})$. S ranges from 0, if f or g vanish, to the maximal value 1, which is obtained if $f = \pm g$.

In a coplanar symmetric (e,2e) setup, the latter is always the case for equal energies of the outgoing electrons, irrespective of the primary energy, the polar emission angles and the choice of the crystal surface. For $f = g$, Eq. (5) is easily seen to become the paradigmatic Bell singlet state.

From Eqs. (4) and (5), one obtains the (e,2e) reaction cross section (intensity)

$$|f - g|^2 \quad \text{and} \quad |f|^2 + |g|^2 \quad (7)$$

for parallel and antiparallel spins, respectively.

If—for given initial conditions—collisions with valence electrons of both spin orientations are possible, the total intensity is the sum of the two terms in Eq. (7), and the final two-electron state is a mixed state described by the sum of the statistical operators corresponding to the two pure states in Eqs. (4) and (5). An appropriate measure of the entanglement is then the "entropy of formation" (e.g., see Ref. [19]):

$$\tilde{S} = S \cdot (|f|^2 + |g|^2)/(|f|^2 + |g|^2 + |f - g|^2), \quad (8)$$

where S is the entropy for the antiparallel-spin case [Eq. (5)], and $|f|^2 + |g|^2$) and $|f - g|^2$ are the intensities for antiparallel and parallel spins [cf. Eq. (7)], respectively. $\tilde{S}$ is thus smaller than S if—in addition to antiparallel spin collisions—there are also collisions between parallel-spin electrons. To create maximal entanglement, one therefore has to choose conditions, under which there are no parallel-spin valence electrons (which is possible in ferromagnets) or under which they are forbidden to contribute to (e,2e) due to selection rules.

Turning now to the issue of how the entanglement in (e,2e) can be studied experimentally, we first note that measuring spin-spin correlations and employing Bell type inequalities is beyond present day technology. Instead, we consider the spin polarization P_3 of the electrons, which leave the surface in one direction (say e_3 in Fig. 1), if the primary electrons are polarized normal to the reaction plane with $P_1 = \pm 1$ (i.e., spin label $\sigma_1 = \pm$). In the case of parallel spin of the valence electron, P_3 is obviously the same as P_1. In the purely antiparallel-spin case, $P_3 = \sigma_1(|f|^2 - |g|^2))/(|f|^2 + |g|^2)$. If valence electrons with both spin orientations contribute, from Eq. (7), one gets

$$P_3 = \sigma_1(|f|^2 - |g|^2 + |f - g|^2)/(|f|^2 + |g|^2 + |f - g|^2). \quad (9)$$

For short, we refer to the numerator (denominator) as intensity difference (total intensity). P_3 is closely related to the entropy $\tilde{S}$ [Eq. (8)] since both are functions of the transition matrix elements f and g. In particular, in the equal energy case ($E_3 = E_4$) with $f = g$, in which the parallel-spin intensity $|f - g|^2$ is zero, we have maximal entanglement $\tilde{S} = 1$ associated with $P_3 = 0$.

In view of making contact with experimental data obtained at a macroscopic distance (about 20 cm) away from the surface, one has to consider the possibility that the entangled pair, which starts at the surface, could suffer decoherence on its way to the detectors due to some interaction with the environment (e.g., see the extensive monographs [20,21] and ample references therein).

Rather than by the wave function, Eq. (5), it would then be represented by a density matrix of the form

$$\rho = \rho_0 + \eta\rho_{\text{int}}, \quad (10)$$

where $\rho_0 + \rho_{\text{int}}$ is the density matrix corresponding to the pure state Eq. (5), ρ_0 respresents an incoherent superposition, and the factor $\eta\epsilon[0,1]$ in front of the interference part ρ_{int} indicates the strength of the decoherence (none for $\eta = 1$ and maximal for $\eta = 0$). The spin polarization P_3 is $\text{tr}[(1\otimes\sigma_z)\rho] = \text{tr}[(1\otimes\sigma_z)\rho_0]$, i.e., the same for any decoherence value η. In particular, for the antiparallel-spin case with maximal entanglement at the surface, the value $P_3 = 0$ would be obtained at the detectors even if the Bell-type state had completely decohered along the way from the surface to the detectors. $P_3 = 0$ is thus a necessary, but by itself not sufficient condition for entanglement at a macroscopic distance.

IV. RESULTS

To get quantitative (e,2e) entanglement results extending beyond the special equal-energy case, numerical calculations for a specific surface system are required. The Cu(111) surface appears most suitable for several reasons. (1) It exhibits a valence electron surface state (so-called Shockley state), which gives rise to strong (e,2e) intensity [10,11]. (2) Since this state is just below the Fermi energy, there are hardly any inelastic multiple scattering events, which would degrade the entanglement. (3) The threefold rotation symmetry of Cu(111) implies a strong dependence of $\tilde{S}$ and P_3 on the azimuthal rotation angle about the surface normal. Applying to Cu(111) a multiple scattering formalism, which has been described in detail in earlier articles (Refs. [22,23] and references therein), we obtained the transition matrix elements f and g and thence the entropy of formation $\tilde{S}$ according to Eq. (8) and the spin polarization P_3 of outgoing electrons e_3 according to Eq. (9). Specific theoretical model features, in particular quasi-particle potentials and the screening of the Coulomb interaction, were taken to be the same as in previous (e,2e) work [24].

In Fig. 2, we present (e,2e) results from Cu(111) calculated for the coplanar symmetric geometry sketched in the upper half of Fig. 1 with fixed polar angles $\vartheta_3 = \vartheta_4 = 45^\circ$. The normally

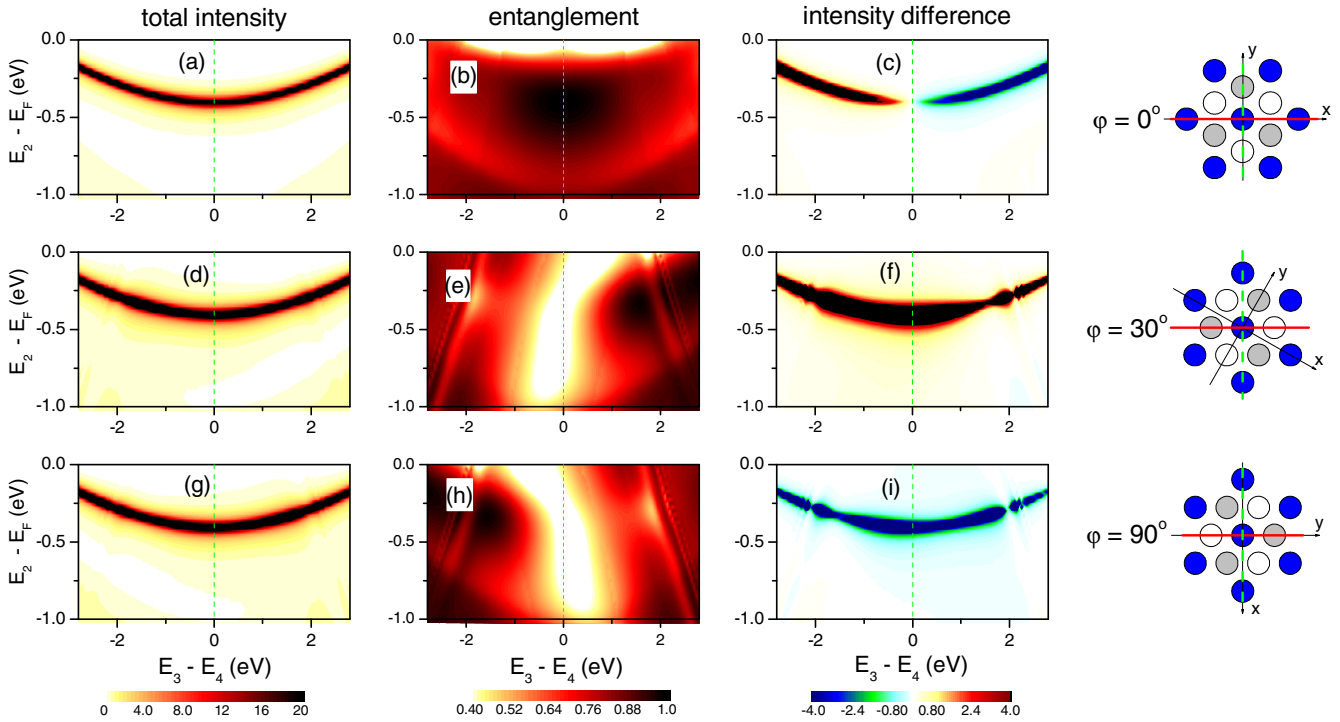

FIG. 2. Theoretical results from Cu(111) for normally incident primary electrons with $E_1 = 24$ eV and spin $\sigma_1 = +$. The two outgoing electrons have energies E_3 and E_4 and equal polar angles $\vartheta_3 = \vartheta_4 = 45°$. Surface geometry sketches are in the right-hand column, the x axis is along the $[1,-1,0]$ direction and the y axis along $[-1,-1,2]$. The red line marks the intersection of the reaction plane with the surface for azimuthal angles $\varphi = 0°$, 30°, and 90° as indicated. The plane normal to the reaction plane (dashed green line) is a mirror plane for $\varphi = 0°$ and a nonmirror plane in the cases $\varphi = 30°$ and 90°. The energy distributions in panels (a)–(i) are presented as functions of the energy difference $E_3 - E_4$ of the two outgoing electrons and of the valence electron energy E_2 minus E_F, which by virtue of energy conservation is equivalent to the sum energy $E_3 + E_4$. In each panel, the vertical dashed line marks the special case of equal energies of the two electrons. (a)–(c) show results for azimuthal angle $\varphi = 0°$. (a) Total intensity $|f|^2 + |g|^2 + |f - g|^2$ [cf. Eq. (7)]. (b) Entropy of formation $\tilde{S}$ [cf. Eq. (8)]. (c) Intensity difference $|f|^2 - |g|^2 + |f - g|^2$, which is equal to the spin polarization P_3 of electrons e_3 in Fig. 1 [cf. Eq. (9)] times the total intensity. (d)–(f) Same as (a)–(c) but for $\varphi = 30°$. (g)–(i) Same as (a)–(c) but for $\varphi = 90°$. The results for $\varphi = 60°$ are not shown, because they are identical with those for $\varphi = 0°$. For primary spin $\sigma_1 = -$, the total intensity and the entropy of formation are the same as for $\sigma_1 = +$, but the intensity difference has the reversed sign.

incident primary electron has fixed energy $E_1 = 24$ eV. Intensities, entropy and spin polarization then depend only on the two outgoing electron energies E_3 and E_4. Since the energy sum $E_3 + E_4$ is equal to $E_1 + E_2$, they can equivalently be regarded as functions of the energy difference $E_3 - E_4$ and the valence electron energy $E_2 + \Phi = E_2 - E_F$ relative to the Fermi energy E_F, where Φ is the work function. Further, in our geometry the conservation laws of Eq. (2) associate with each pair (E_3, E_4) a unique value of valence electron parallel-momentum $\vec{k}_2^{\parallel} = (k_{2r}, 0)$, where k_{2r} is the component in the reaction plane. In particular, electrons with $E_3 - E_4 = 0$ originate from collisions with valence electrons with $\vec{k}_2^{\parallel} = (0,0)$, i.e., at the center of the surface Brillouin zone. The presentation of (e,2e) results as functions of $E_3 - E_4$ and $E_2 - E_F$ thus facilitates the association of individual (e,2e) intensity features with features of the underlying $\vec{k}^{\parallel}$-resolved valence electron density of states. Figure 2(a) shows, for the reaction plane at azimuthal angle $\varphi = 0°$ (cf. geometry sketch in Fig. 2), the total intensity $|f|^2 + |g|^2 + |f - g|^2$ [cf. Eq. (7)] arising from collisions of primary spin-up electrons with both spin-up and spin-down valence electrons. The dominant feature is the arched structure, which from a valence energy of about 0.4 eV below the Fermi energy E_F at $E_3 - E_4 = 0$ disperses upward towards E_F. This structure reflects the dispersion of the sp-like Shockley surface state (cf. Ref. [9] and references therein). For studying entanglement, this state has the important virtue of even symmetry with respect to mirror planes normal to the surface. If such a mirror plane exists normal to the chosen (e,2e) reaction plane, selection rules dictate that for $E_3 = E_4$ the parallel-spin intensity [Eq. (7)] is zero and cannot degrade entropy and spin polarization [25]. As the geometry sketch in the first row of Fig. 2 indicates, this is the case for $\varphi = 0°$. Consequently, at the bottom of the Shockley state arch, the entropy in Fig. 2(b) has the maximal value one. The intensity difference shown in Fig. 2(c) and the spin polarization P_3 [cf. Eq. (9)] are zero. Sizeable entropy values are seen to extend out to about $E_3 - E_4 = \pm 2$ eV. Going away from the center, the intensity difference and P_3 become finite, with opposite sign.

For azimuthal angles $\varphi = 30°$ [second row of Fig. 2 and $\varphi = 90°$ (third row)], the plane normal to the reaction plane is not a mirror plane. Consequently, collisions between parallel-spin electrons will generally contribute a nonzero intensity term $|f - g|^2$. While the total intensity [Figs. 2(d) and 2(g)]

is only mildly affected, entropy and intensity difference are changed drastically. In both Figs. 2(e) and 2(h), $\tilde{S}$ is seen to be strongly reduced in the central region of the Shockley arch, and the intensity difference [in Figs. 2(f) and 2(i)] is now large, with opposite signs for $\varphi = 30^\circ$ and $\varphi = 90^\circ$. For the spin polarization P_3 [Eq. (9)], which is the intensity difference divided by the total intensity, this means that—in contrast to crossing zero at $E_3 - E_4 = 0$ in the case $\varphi = 0^\circ$—it has sizable positive (negative) values for $\varphi = 30^\circ$ ($\varphi = 90^\circ$).

The relation between entropy and spin polarization can be explicitly demonstrated over the entire $(E_3 - E_4)$ range by noting that in the valence energy range between E_F and -1 eV, which is accessible in our experiment with energy resolution of 1 eV, the intensity is concentrated in the Shockley arch [cf. Figs. 2(a), 2(d), and 2(g)]. Weighted averages $\overline{S}$ of $\tilde{S}$ and $\overline{P}_3$ of P_3 over this E_2 interval, which are both functions of $E_3 - E_4$, therefore essentially represent entropy and spin polarization along the Shockley arch. $\overline{S}(E_3 - E_4)$ and $\overline{P}_3(E_3 - E_4)$ were calculated from Eqs. (8) and (9), respectively, by integrating the numerator and denominator separately over the valence energy interval E_2 from -1.0 eV up to the Fermi level.

In Fig. 3, we show $\overline{S}$ and $\overline{P}_3$ for the azimuthal angles $\varphi = 0^\circ, 30^\circ$, and 90°. For comparison, we include the corresponding quantities $\overline{S}^{\rm ap}$ and $\overline{P}_3^{\rm ap}$ for the case of antiparallel spins only, which were obtained in the same way from Eqs. (8) and (9) but without the parallel-spin intensity term $|f - g|^2$. In Fig. 3(a), we show results for azimuthal angle $\varphi = 0^\circ$, for which the plane normal to the reaction plane is a mirror plane. Most notably, for equal energy sharing $E_3 - E_4 = 0$ the entanglement measure $\overline{S}$ attains the maximally possible value 1, whereas the spin polarization $\overline{P}_3$ crosses through zero. $\overline{S}^{\rm ap}$ and $\overline{P}_3^{\rm ap}$ are the same as $\overline{S}$ and $\overline{P}_3$, since for equal energy sharing parallel-spin contributions are forbidden by selection rule. This still holds in very good approximation in the range between about -0.5 and 0.5 eV. Below about -1 eV and above about 1 eV, parallel-spin contributions, which for the present positive primary spin polarization are positive, have shifted $\overline{P}_3$ upwards with respect to $\overline{P}_3^{\rm ap}$ and reduced $\overline{S}$ with respect to $\overline{S}^{\rm ap}$. This upward shift deprives $\overline{P}_3$ of the antisymmetry, which $\overline{P}_3^{\rm ap}$ exhibits.

The results for $\varphi = 30^\circ$ [Fig. 3(b)] and $\varphi = 90^\circ$ [Fig. 3(c)], for which the plane normal to the reaction plane is not a mirror plane, are strikingly different. At $E_3 - E_4 = 0$, the entanglement measure $\overline{S}$ is minimal and the polarization has no zero crossing. In fact, $\overline{P}_3$ is positive (negative) throughout the entire energy range for $\varphi = 30^\circ$ ($\varphi = 90^\circ$). $\overline{S}$ and $\overline{S}^{\rm ap}$ for $\varphi = 30^\circ$ and 90° are seen to be related by a reflection at $E_3 - E_4 = 0$. The two $\overline{P}_3^{\rm ap}$ curves are transformed into each other by reflection and sign reversal. These properties are a due to the fact that the plane at $\varphi = 60^\circ$ is a mirror plane.

As demonstrated above, the entanglement of the electron pairs is very closely associated with the spin polarization P_3 of the electrons leaving the Cu surface in one direction. Since the sign of P_3 is reversed by reversing the sign σ_1 of the primary electron spin, P_3 can be measured as the asymmetry after spin-dependent reflection at the spin-polarizing mirror, see Fig. 1.

Experimental spin polarization data are presented, together with theoretical results, in Fig. 4. Due to experimental

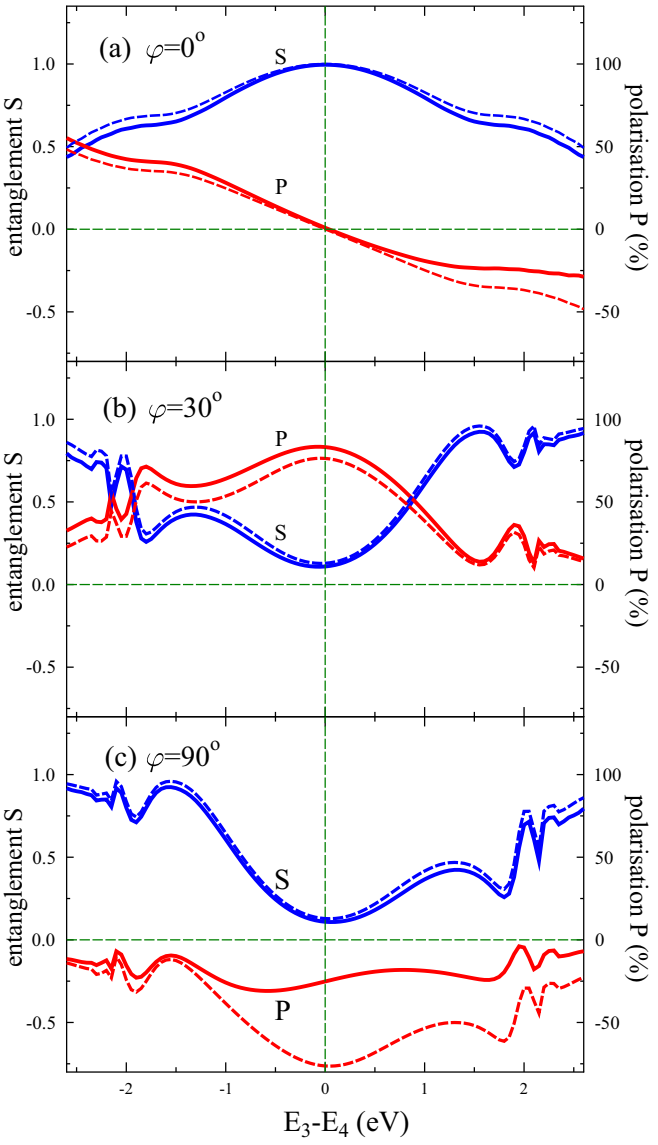

FIG. 3. Weighted averages $\overline{S}$ of entropy (solid blue lines) and $\overline{P}_3$ of spin polarization (solid red lines), which were—for the same conditions as the results in Fig. 2—obtained by integrating the numerators and denominators of Eqs. (8) and (9), respectively, over the valence energy interval from -1.0 eV up to the Fermi level. Neglecting the parallel-spin intensity term $|f - g|^2$, this procedure yields the corresponding quantities $\overline{S}^{\rm ap}$ (dashed blue lines) and $\overline{P}_3^{\rm ap}$ (dashed red lines) for antiparallel spins only. (a)–(c) show the results for the azimuthal angles $\varphi = 0^\circ$, 30°, and 90°. Results for $\varphi = 60^\circ$ are the same as those for $\varphi = 0^\circ$.

energy resolution, these data have been collected over an energy interval ΔE_2 of 1 eV below the Fermi energy, which comprises the Shockley surface state, and a number of intervals $\Delta(E_3 - E_4)$. The corresponding theoretical results are the average polarization curves $\overline{P}_3(E_3 - E4)$, which were calculated from Eq. (9) by averaging the intensity difference (numerator) and the total intensity (denominator) separately over the valence energy interval E_2 from -1.0 eV up to the Fermi level. In Fig. 4(a), we show results for azimuthal angle $\varphi = 0^\circ$, for which the plane normal to the reaction

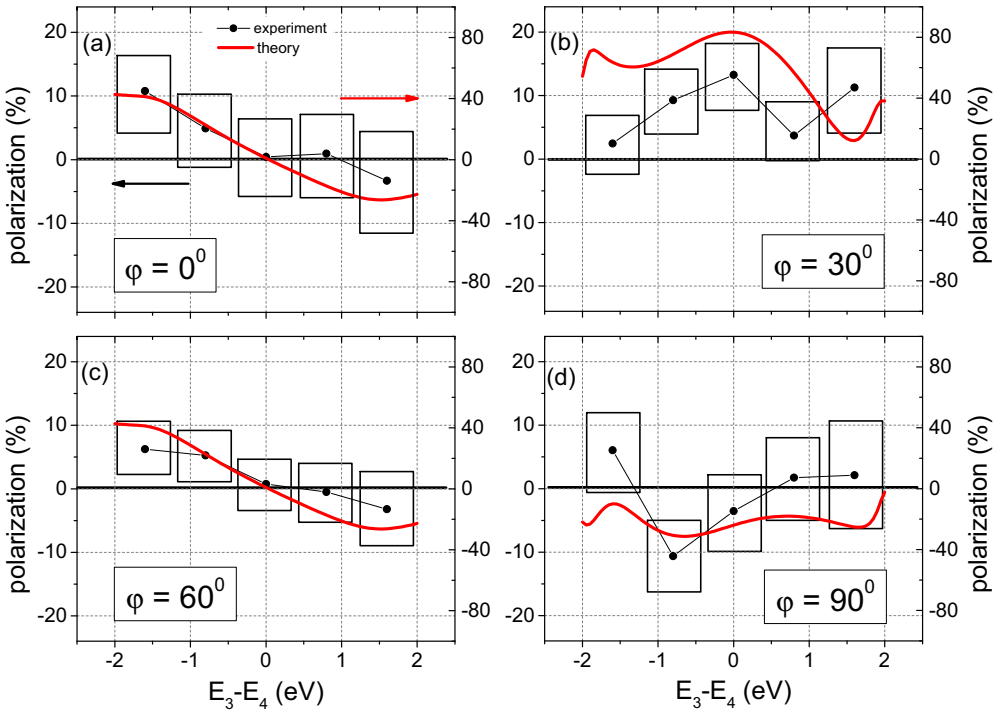

FIG. 4. Spin polarization P_3 as a function of the energy difference $E_3 - E_4$ for different azimuthal angles φ for primary energy $E_1 = 24$ eV. The theoretical results (solid red lines) were obtained, for primary spin $\sigma_1 = +$, from Eq. (9) by averaging over the valence energy interval E_2 from -1 eV up to E_F, which includes the entire Shockley surface state. The experimental results are represented by fat dots inside a rectangle. The horizontal extension indicates the energy integration range. The vertical extension is the statistical uncertainty at each dot. The experimental (theoretical) polarization scale is on the left (right). The constant scaling factor between them takes into account various depolarization effects.

plane is a mirror plane. The salient common feature of the experimental and theoretical polarization is the zero crossing at $E_3 - E_4 = 0$. As shown in Fig. 3(a), at this point the entanglement measure $\overline{S}$ reaches its maximal value 1. Our experimental result is therefore consistent with the generation of maximally entangled electron pairs. This is the central result of the present work.

As a cross-check, we show in Fig. 4(c) experimental data obtained at $\varphi = 60°$, which according to symmetry arguments as well as numerical calculations should be identical to those for $\varphi = 0°$. The results for $\varphi = 30°$ [Fig. 4(b)] and $\varphi = 90°$ [Fig. 4(d)], for which the plane normal to the reaction plane is not a mirror plane, are strikingly different. The polarization has no zero crossing, but is positive (negative) throughout for $\varphi = 30°$ ($\varphi = 90°$). As can be seen in Figs. 3(b) and 3(c), the entanglement measure $\overline{S}$ has a minimum of 0.12 at $E_3 - E_4 = 0$ in contrast to the maximal value 1 obtained for $\varphi = 0°$.

The experimental polarization values are about a factor 4 smaller than the theoretical values. A contributing factor of this reduction arises from random coincidences. These are events in which two primary electrons individually cause single-electron emission. Our coincidence circuit will also register these events. The spin polarization of random coincidences is expected to vanish. The intensity contribution of this pathway can be adjusted by the primary flux. It is well-known that random coincidences scale quadratically with the flux, while the intensity of interest (true coincidences) scale linearly with flux. We adjusted the flux such that the ratio of true to random coincidences is of the order of one. In this case, the observed spin polarization is reduced by a factor of about 2 compared to the spin polarization of the true coincidences.

As explained above, the measured spin polarization in Fig. 4(a) would be the same if the pair state, which is strongly entangled at the surface, had decohered along the way to the detectors due to interaction with the environment. As interaction mechanisms, which in our apparatus might reduce the spin entanglement, we consider collisions with rest gas molecules and magnetic fields. Since the base pressure in our vacuum chamber is less than 10^{-10} mbar, the mean free path for collisions between rest gas molecules is more than 10^6 m. The mean free path for electron-molecule collisions is therefore certainly much larger than the electron trajectories and such collisions will hardly cause decoherence. As for magnetic fields, we have shielded the earth magnetic field by compensating coils and by mu-metal such that the field inside our chamber is only 1 mG. It seems rather unlikely that such a weak magnetic field can significantly impair the entanglement.

V. CONCLUSION

We performed (e,2e) experiments on a Cu(111) surface and focused on the events which included the Shockley surface state. If we select a particular sample alignment with respect to the scattering plane ($\varphi = 0°$) our experimental results are consistent with an entanglement of two electrons at a macroscopic distance. Estimating decoherence due to

interactions along the way as small, we moreover regard it as very likely that they are actually significantly entangled. For a definite verification, however, one has to await a new generation of experiment with a spin detector in each arm allowing the measurement of correlations and thence the violation of Bell-type inequalities.

[1] A. Einstein, B. Podolsky, and N. Rosen, Phys. Rev. **47**, 777 (1935).

[2] E. Schrödinger, Proc. Cambridge Philos. Soc. **31**, 555 (1935); **32**, 446 (1936).

[3] J. F. Clauser and A. Shimony, Rep. Prog. Phys. **41**, 1881 (1978).

[4] M. D. Reid, P. D. Drummond, W. P. Bowen, E. G. Cavalcanti, P. K. Lam, H. A. Bachor, U. L. Andersen, and G. Leuchs, Rev. Mod. Phys. **81**, 1727 (2009).

[5] R. Horodecki, P. Horodecki, M. Horodecki, and K. Horodecki, Rev. Mod. Phys. **81**, 865 (2009).

[6] L. Lamata and J. Leon, Phys. Rev. A **73**, 052322 (2006).

[7] O. M. Artamonov, S. N. Samarin, A. N. Vetlugin, I. V. Sokolov, and J. F. Williams, J. Electron Spectrosc. Relat. Phenom. **205**, 66 (2015).

[8] R. Feder, F. Giebels, and H. Gollisch, Phys. Rev. B **92**, 075420 (2015).

[9] R. Courths, M. Lau, T. Scheunemann, H. Gollisch, and R. Feder, Phys. Rev. B **63**, 195110 (2001).

[10] F. O. Schumann, R. S. Dhaka, G. A. van Riessen, Z. Wei, and J. Kirschner, Phys. Rev. B **84**, 125106 (2011).

[11] F. O. Schumann, C. Winkler, and J. Kirschner, Phys. Rev. B **88**, 085129 (2013).

[12] F. O. Schumann, C. Winkler, J. Kirschner, F. Giebels, H. Gollisch, and R. Feder, Phys. Rev. Lett. **104**, 087602 (2010).

[13] Y. A. Mamaev, L. G. Gerchikov, Y. P. Yashin, D. A. Vasilyev, V. V. Kuzmichev, V. M. Ustinov, A. E. Zhukov, V. S. Mikhron, and A. P. Vasiliev, Appl. Phys. Lett. **93**, 081114 (2008).

[14] J. Kirschner, F. Giebels, H. Gollisch, and R. Feder, Phys. Rev. B **88**, 125419 (2013).

[15] D. Vasilyev, C. Tusche, F. Giebels, H. Gollisch, R. Feder, and J. Kirschner, J. Electron Spectrosc. Relat. Phenom. **199**, 10 (2015).

[16] C. Tusche, A. Krasyuk, and J. Kirschner, Ultramicroscopy **159**, 520 (2015).

[17] J. Schliemann, J. I. Cirac, M. Kuś, M. Lewenstein, and D. Loss, Phys. Rev. A **64**, 022303 (2001).

[18] G. C. Ghirardi and L. Marinatto, Phys. Rev. A **70**, 012109 (2004).

[19] C. H. Bennett, D. P. DiVincenzo, J. A. Smolin, and W. K. Wootters, Phys. Rev. A **54**, 3824 (1996).

[20] M. Schlosshauer, *Decoherence and the Quantum-to-Classical Transition* (Springer, Berlin, Heidelberg, 2008).

[21] *Entanglement and Decoherence: Foundations and Modern Trends*, edited by A. Buchleitner, C. Viviescas, and M. Tiersch, Lecture Notes in Physics 768 (Springer, Berlin, Heidelberg, 2009).

[22] R. Feder and H. Gollisch, in *Solid State Photoemission and Related Methods*, edited by W. Schattke and M. A. van Hove (Wiley-VCH, Weinheim, 2003), Chap. 9.

[23] H. Gollisch, N. V. Schwartzenberg, and R. Feder, Phys. Rev. B **74**, 075407 (2006).

[24] F. Giebels, H. Gollisch, and R. Feder, J. Phys.: Condens. Matter **21**, 355002 (2009).

[25] R. Feder and H. Gollisch, Solid State Commun. **119**, 625 (2001).